

Interplay between structure and magnetism in hydride iron-vanadium systems

A. Lebon,¹ A. Mokrani,² and A. Vega^{2,*}

¹LMB/UBO, 6 Avenue Victor Le Gorgeu, 29285 Brest Cedex, France

²Institut des Matériaux Jean Rouxel, UMR CNRS 6502, Université de Nantes, 2 rue de la Houssinière, B.P. 44322 Nantes, France

(Received 23 July 2008; revised manuscript received 24 September 2008; published 4 November 2008)

The structural and electronic properties of dimers, bulk, and alloys of Fe and V upon loading with hydrogen have been investigated using the density-functional method Spanish Initiative for Electronic Simulation of Thousand of Atoms. We have calculated the hydrogen-induced modifications of both the geometrical structure and the magnetic properties, which have been found to be closely related to each other. The general trends derived from our results are in good agreement with those found in the experimental characterizations of hydrogen-loaded Fe/V multilayer systems. In particular, we have found that hydrogen prefers a V environment when inserted in the alloy systems at high concentration; it occupies octahedral positions leading to a strong anisotropic expansion of the lattice accompanied by an increase in the local Fe magnetic moments. We have found that the main trends obtained in the extended systems were already present in the most stable geometrical and spin isomers of the freestanding FeVH clusters.

DOI: [10.1103/PhysRevB.78.184401](https://doi.org/10.1103/PhysRevB.78.184401)

PACS number(s): 75.10.Lp, 71.20.Be, 75.75.+a

I. INTRODUCTION

The understanding and prediction of the structural and electronic properties of systems composed by a ferromagnetic (FM) and an antiferromagnetic (AFM) [or nonmagnetic (NM)] metal is one of the hot topics in materials science and nanotechnology. Such systems can be grown at present in a variety of forms, ranging from the finite-size regime (binary clusters) to the extended regime (overlayers, multilayers, and alloys). The fundamental knowledge of their structural properties—which depend on the relative concentration, type of bonding, and possible mismatch, as well as their electronic properties (magnetism, optical properties, transport)—is one of the aspects that justifies the interest in these systems. Besides, the possibility of tailoring those properties for technological purposes has opened new prospects in the development of nanostructured devices that improve our daily life.

Examples of the above phenomena are, for instance, the cooperative effect in clusters composed by FM and AFM elements that give rise to an enhancement of the magnetic moment when whole cluster has FM order (depending on the relative concentration of the FM and AFM elements) with possible application as magnetic units in dense magnetic storage devices or, in the context of spin-dependent transport, the giant magnetoresistance (used in spin filters, magnetic random access memories, among other systems), which is related to the interlayer exchange coupling (IEC) across a spacer.¹⁻³ The possibility of tuning the magnetic and transport properties of these systems provides a way to design more specific devices. This has been shown for instance in the multilayers through either alloying^{4,5} the spacer with another metal or inserting hydrogen.⁶ The hydrogen loading opens a route to tailor real two-dimensional magnetic systems as it is suggested through neutron reflectivity measurements.⁷ In Fe₂/V₁₃ multilayers, where small amount of hydrogen (less than 5%) is inserted, a change in sign of the IEC (J_{\perp}) from FM to AFM takes place for a critical H concentration. At the critical FM to AFM transition, J_{\perp} is

expected to cancel out, and the magnetic coupling is confined within the two-dimensional Fe layers, which are decoupled to each other. Furthermore, the insertion of H is also accompanied by an increase in the total moment localized on the iron atoms.⁸ Last but not least, the H loading is shown to be a reversible process.

A calculated chemical binding energy of a pair of hydrogen atoms, located at tetrahedral (T) sites in V, shows a strong H-H repulsion when they are at first nearest neighboring positions; the stability is obtained when the two atoms of hydrogen are at fourth nearest neighboring positions.⁹ These results are in accord with Switendick criterion,¹⁰ which states that in metal hydride solid solution two hydrogen atoms cannot come closer than 2.1 Å. The position of H seems to play an important role in the behavior of the system, and some trends have been experimentally established.¹¹ The H loading at high concentration produces an expansion of the lattice in the direction perpendicular to the interface plane.¹² Hydrogen atoms are absorbed in interstitial positions within the vanadium layers; they occupy octahedral (O) sites in the vanadium layers enforced by the mechanical constraints in the films. Hydrogen atoms stay far from the iron layers. The vanadium layers are also suggested to undergo a structural phase transition to the β phase of vanadium hydride as increasing the H content, according to the extended x-ray absorption fine structure (EXAFS) data.¹³

On the theoretical side concerning Fe/V systems, most of the studies have focused on the magnetic profiles in multilayers,^{14,15} and few of them have considered the presence of H. Ostanin *et al.*¹⁶ using full-potential linear muffin-tin orbital (FP-LMTO) studied the magnetic behavior at the interface and the resistivity as a function of the H concentration in the V layer. The moment at the interface is supposed to decrease due to the important tetragonal distortion subsequent to the H absorption, although structural relaxation was not considered. Duda and co-workers¹⁷ combined a FP-LMTO study with x-ray emission spectroscopy (XES) at the L edge of vanadium in Fe₁₄/V₁₃ to show that H states hybridize with the 3d electrons of V. The FP-LMTO calculations were also carried out without relaxation. Full relaxation

was considered within the pseudopotential plane-wave Vienna *Ab Initio* Simulation Package (VASP) calculations of Meded and co-workers¹⁸ to derive information on the conductivity. They concluded that the change in the conductivity was solely caused by a volume change. The above density-functional theory (DFT) studies considered ideally smooth interface. Uzdin *et al.*¹⁹ used the periodic Anderson model to analyze the role of Fe-V intermixing on the increase in the magnetic moment at the interface (without structural relaxation). Due to intermixing, the global magnetic moment was lower than expected in H-free superlattices. On the contrary, the addition of H leads to a magnetic moment larger than the one predicted if assuming ideally smooth interfaces.

In view of the above results, it is evident that the general trends experimentally observed in Fe-V systems (i.e., the preference of H to locate itself in a V environment rather than in a Fe environment, the increase in the Fe moment, and the lattice expansion upon H loading) are closely related to each other, and a systematical theoretical study of Fe-V-H in different environments is pertinent to provide theoretical support. Moreover such theoretical study should be preferably carried out within state of the art DFT approach and considering full relaxation in order to search for the most stable structural and electronic configuration, from which those trends should be evidenced. The DFT code Spanish Initiative for Electronic Simulation of Thousand of Atoms (SIESTA) fulfils such requirements, although its use, in the fully unconstrained version, for a full systematic study of the complex superlattices experimentally grown as a function of H loading is at present a huge computational task due to the large supercells required and the many input configurations to test, particularly for intermediate H concentrations. The aim of the present work is to show how the general trends described above in the case of Fe/V multilayers can be found in Fe-V-H systems with different environments, like in the finite-size regime of freestanding clusters or in the bulk limit of alloys. The Fe-V dimer can be seen as the molecular realization of a B2 alloy, and the study of these systems is possible to be performed in the framework of a fully unconstrained DFT approach.

In the next section we describe the DFT approach used for the calculation. Section III is devoted to the freestanding clusters FeVH for which we determined all possible structural and spin isomers. In Sec. IV we discuss the results obtained for the B2 FeV alloy upon H loading, in which we also determined all the possible structural and spin configurations. The last section summarizes our main conclusions.

II. THEORETICAL MODEL AND COMPUTATIONAL DETAILS

In the present calculations for the freestanding clusters and extended systems of Fe and V, we have used the DFT pseudopotential code SIESTA (Ref. 20) which employs linear combination of pseudoatomic orbitals as basis sets. We have used for the exchange and correlation potential the GGA parameterized by Perdew, Burke and Ernzerhof.²¹ The atomic core has been replaced by a nonlocal norm-conserving Troullier-Martins²² pseudopotential that is factor-

ized in the Kleinman-Bylander form.²³ The ionic pseudopotentials were generated using the following electronic configurations: $3d^7, 4s^1$, and $4p^0$ for Fe and $3d^3, 4s^2$, and $3p^6$ for V. Notice that the semicore $3p$ states have been taken out of the V core (and considered explicitly in the basis) since this has been shown to considerably improve the description of the magnetic trends in semi-infinite V systems.^{24,25} In addition, the insertion of this semicore states in the pseudopotential generation improved our evaluation of the V-V distance that has been found otherwise to be too short and physically inconsistent. The Fe pseudopotential was generated from an excited electronic configuration of the atom. This pseudopotential is known to reproduce the experimental moment of Fe₂ as previously reported by Izquierdo *et al.*²⁶ The s, p , and d cutoff radii were 2.00, 2.00, and 2.00 a.u. for Fe and 2.50, 2.17, and 0.90 a.u. for V. We have included nonlinear core corrections to account for the overlap of the core charges with the valence d orbitals. The matching radius for the core corrections was 0.70 a.u. for Fe and 1.2 a.u. for V.²⁷ We have tested that these pseudopotentials reproduced accurately the eigenvalues of different excited states of the respective isolated atoms.

Concerning the basis set and the energy cutoff to define the real-space grid for numerical calculations involving the electron density, a detailed and careful test has been performed. Finally, we have described the valence states using double ζ -polarized basis functions, further referred to as DZP, with two orbitals having different radial form to describe both the $4s$ and the $3d$ shells of Fe, being the $4s$ single polarized. In the case of V, two orbitals having different radial form were taken to describe the $3p, 4s$, and $3d$ valence states, being the $4s$ single polarized. Notice that polarization of the $4s$ states leads to the inclusion of one orbital of $4p$ type in the basis set. We have considered an electronic temperature of 15 meV and a 350-Ry energy cutoff to define the real-space grid for numerical calculations involving the electron density. (We have tested triple ζ basis set, larger cutoffs, and lower electronic temperature for particular cases and verified that they do not substantially modify the results.)

The code allows performing, together with the electronic calculation, structural optimization using a variety of algorithms. To optimize the geometrical structures in the freestanding Fe-Fe, V-V, and Fe-V dimers, with and without H, we have performed a full relaxation using the conjugate gradient algorithm, starting from all the possible initial structures, with axial and triangular shapes and with H at the different possible positions. We have also considered both parallel (P) and antiparallel (AP) magnetic couplings within the clusters. In the case of the bulk and alloys, we have also performed a relaxation considering the H located in the different tetrahedral and octahedral interstitial sites in the system. The structural optimization was stopped when each force component at each atom was smaller than 1 meV/Å.

Spin-orbit interaction is not considered in the calculations so that the possible magnetocrystalline and interface anisotropies are not taken into account. Therefore, the absolute direction of the local magnetic moments is not defined, but only their relative orientation.

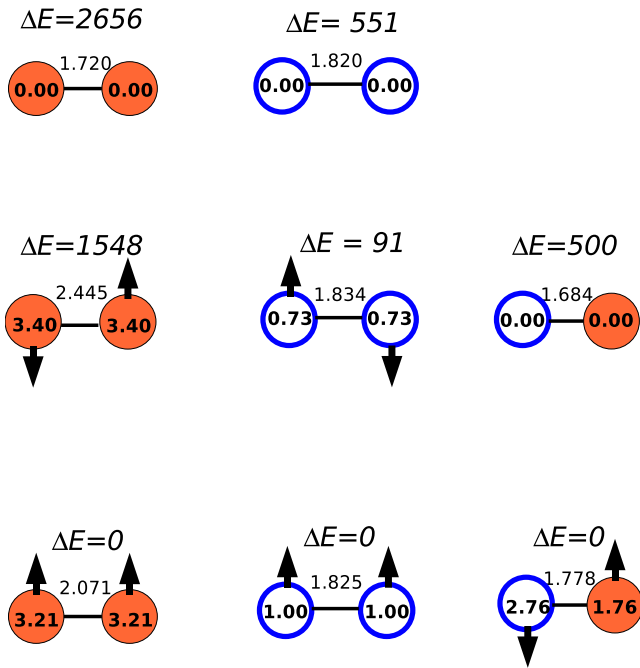


FIG. 1. (Color online) Structural and magnetic configurations obtained for the freestanding dimers Fe-Fe, V-V, and Fe-V represented in the first, second, and third column, respectively. The Fe atoms are represented by the orange filled circles and the V by the blue empty circles. Inside the circles are given the local magnetic moments in units of Bohr magneton and the couplings represented with arrows. In each column ΔE gives the total energy difference (in units of meV) with respect to the ground state (bottom of the column). Interatomic distances (in Å) are indicated between the circles representing the atoms.

III. FREESTANDING ATOMIC CLUSTERS

In order to better understand the structural and magnetic behavior of the Fe-V dimer upon H loading, we have first calculated the most stable configurations of the H-free dimers Fe-Fe, V-V, and Fe-V. In Fig. 1 we show the ground state, as well as the different isomers of these systems. As expected, they have shrunk interatomic distance with respect to the bulk. The ground state of the homonuclear dimers P magnetic coupling. The AP excited state of the Fe dimer is about 1548 meV less stable than the P ground state, whereas in the V dimer the difference amounts to 90 meV. By contrast, the ground state of the Fe-V dimer has clearly AP magnetic order, the P state is not found as solution, and the NM configuration is 500 meV above the AP one. Therefore, in the atomic limit we already find the magnetic trends experimentally observed and theoretically calculated in the multilayers, i.e., ferromagnetic coupling in Fe and antiferromagnetic coupling at the Fe/V interface.^{14,15} But we also obtain some differences such as the larger local magnetic moments characteristic of the atomic limit, which in the case of homonuclear V dimer lead to a magnetic ground state by contrast to the paramagnetic state of its bulk counterpart.

Let us now present the results obtained for the H-loaded dimers. We have considered all the possible positions of the H atom with respect to each dimer, and we have fully relaxed the system. Here we also considered the P, AP, and NM

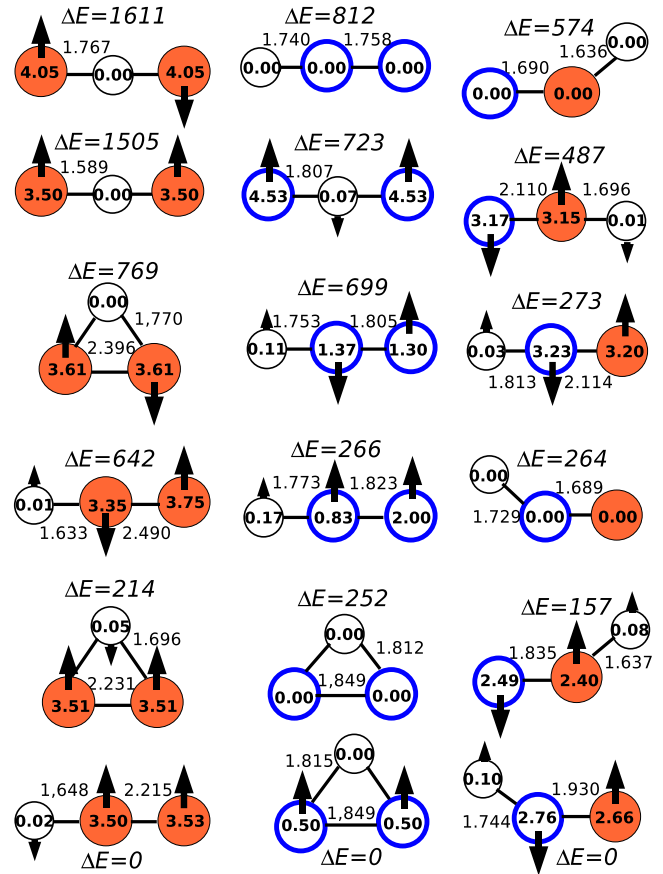


FIG. 2. (Color online) Structural and magnetic configurations obtained for the freestanding H-loaded dimers Fe-Fe, V-V, and Fe-V, represented in the first, second, and third column, respectively. Orange filled, blue empty, and small black circles represent the Fe, V, and H atoms, respectively. Inside the circles are given the local magnetic moments in units of Bohr magneton and the couplings represented with arrows. In each column ΔE gives the total energy difference (in units of meV) with respect to the ground state (bottom of the column). Interatomic distances (in Å) are indicated between the circles representing the atoms.

configurations. In Fig. 2 we show the ground state, as well as the five lowest energy isomers of the clusters FeFeH, VVH, and FeVH. The following general trends can be inferred (see Figs. 1 and 2):

- (i) the H atom stays in a V-rich environment.
- (ii) no change in the magnetic order in the dimers is obtained upon H loading.
- (iii) the H loading in the dimers leads to an increase in the interatomic distance and to an enhancement (reduction) in the local magnetic moment of the Fe (V) atom.

The general trend (i) is supported by the following results. The most stable position of H in the Fe-Fe dimer is the one which minimizes the interaction with Fe by forming an axial trimer with H outside the dimer. Less stable isomers are found with H located in between the Fe atoms. On the contrary, in the V-V dimer, the H atom maximizes its interaction with both V atoms forming a triangle. Finally, in the Fe-V dimer, H stays at the vanadium side rather than at the Fe side. Here we found several isomers close in energy but those with H located between Fe and V are considerably less

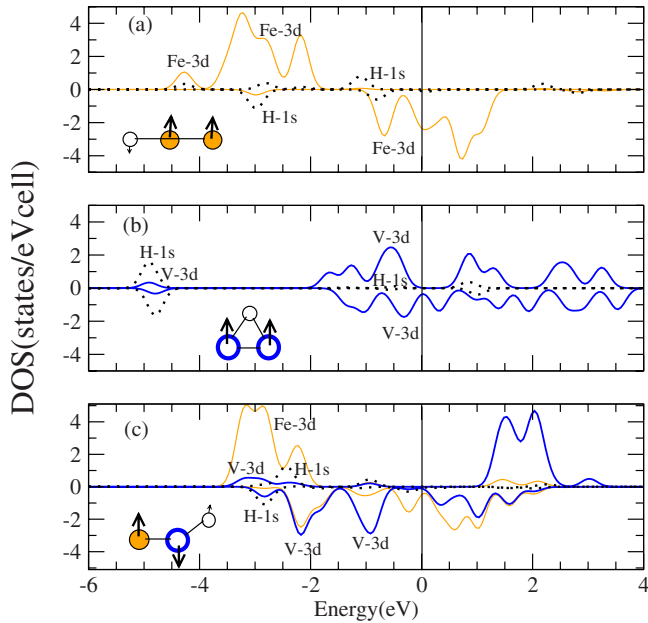


FIG. 3. (Color online) Orbital-projected densities of states for the ground-state configurations of the H-loaded dimers shown in Fig. 2. The thin orange solid lines correspond to the 3d orbitals of Fe, while the thick blue solid line is for V. The dashed thick black lines correspond to the 1s orbital of H.

stable. These results are consistent with the experimentally observed tendency of H to be absorbed in the V layers of FeV multilayers instead of in the Fe layers or at the interface.¹¹ In Fig. 3 we show the orbital-projected densities of states for the ground-state H-loaded dimers. In the H-loaded V dimer, we find a structure at -5 eV in which the 3d states of V hybridize with the 1s state of H [Fig. 3(b)]. This feature is not obtained when we have a Fe atom [Fig. 3(a) and 3(c)]. A similar feature was experimentally observed at about -8 eV through XES in $\text{Fe}_{13}\text{V}_{14}$ multilayers and was interpreted as a result of the hybridization of the 3d states of vanadium and the 1s state of hydrogen,¹⁷ an indication of the H insertion within the V layers.

Concerning the magnetic order in the H-loaded dimers, general trend (ii), we see from Figs. 1 and 2 that the most stable isomers of the H-loaded Fe-Fe dimers have P magnetic coupling with AP isomers 640 meV above the P one. The strong P coupling in Fe is reflected in the fact that a triangular P isomer (with H bonded to both Fe atoms) is more stable than an AP axial isomer (with H outside the dimer). Thus, magnetism is a driving force in the Fe dimers. V has no such strong magnetic coupling and the structural contribution dominates. The P one being the ground state also when H is attached (as in the H-free dimers) but becomes the axial isomer with P coupling considerably less stable. The importance of the structural contribution is further illustrated by the greater stability of the NM V-V-H triangle as compared to the P configuration of the axial cluster. Finally, in the H-loaded Fe-V dimer, the AP coupling between Fe and V is preserved.

These results give further support to the close relation between structure and magnetism in low-dimensional systems, and show that the relative contribution of the magnetic

effects to the total energy of the system depends on the involved transition-metal elements. Besides, it proves that a full-relaxed electronic structure calculation is required in order to find the most stable structural and spin isomer. It is remarkable that again these general trends are consistent with those experimentally observed in both H-free and H-loaded Fe/V multilayers, for which strong AP magnetic coupling was found at the Fe/V interface.

The general trend (iii), concerning the influence of H on the interatomic distances and on the magnetic moments, is illustrated in Fig. 2. The Fe-V interatomic distance in the ground state of the H-loaded Fe-V dimer is larger than in the H-free Fe-V dimer, and this is accompanied by an increase in the local moment in Fe. The enhancement of the local magnetic moment in Fe occurs for all the configuration with AP magnetic order. The increase in the Fe-V distance is more pronounced when H is adsorbed on the V side. This general trend obtained for the H-loaded Fe-V dimers is consistent with the experimentally observed increase in the lattice parameter in Fe/V multilayers upon H loading at intermediate and high concentrations.¹¹

IV. BULK ENVIRONMENTS

Similar trends as those obtained in the freestanding clusters can be discussed in the extended regime of bulk and alloys. In Table I we summarize the results for these systems. Let us consider at first the case of Fe and V bulks upon hydrogen insertion in either the T or O sites. In all cases we have fully relaxed the structures. Within V bcc, H is found to be absorbed preferentially in the T site, which leads to an isotropic expansion of the unit cell. For the same H concentration of $x=0.5$ the computed expansion coefficient that amounts to 11% compares remarkably well with the experimental expansion coefficient of 10% (see Fig. 4 of Ref. 11). This is at odd with the results obtained for Fe bcc in which the O position of H is favored over the T one, and it is accompanied by a large anisotropic tetragonal expansion. The insertion of H atoms in V is a long standing issue as it is possible to store a great amount of H within bulk V or V slabs.²⁸ A complex sequence of the H insertion and related phase transitions is described by Bloch *et al.*²⁹ who studied the H absorption in a 50-nm V film deposited on a Fe buffer supported on a MgO substrate. The insertion of H in the T sites (as obtained in our calculations) was observed experimentally in the first stage of the H absorption. For higher H concentration, the H-H interaction seems to favor the insertion of H in O sites. A subsequent huge lattice expansion of roughly 10%, characterized through x-ray diffraction (XRD), seems to be associated with the insertion in the O site. The insertion in the O sites is triggered once the H concentration has reached $x=\text{H}/\text{V} > 0.15-0.30$.^{29,30} This latter type of insertion has been described as unstable against a phase transition toward the β phase of vanadium according to EXAFS data.¹³ We note that in this β phase of V_2H the O site is highly distorted, being the H atom no longer aligned with the V atoms in the plane. Such local structure resembles the triangular configuration obtained as the ground state in the H-loaded V dimer. Our results for the clusters are thus con-

TABLE I. Optimized cell parameters (in Å) and local magnetic moments (in μ_B) obtained in the bulk systems. The first row concerns the pure Fe bulk, followed by the results for the H-loaded Fe bulk for the different interstitial sites of H. The fourth, fifth, and sixth rows concern the pure V bulk and the H-loaded V bulk. B2 (Fe+V) indicates the H-free B2 alloy. The six last rows concern the H-loaded alloy, the first three of which correspond to the cell-relaxed case, while the three others are for the optimized cell when fixing the in-plane distance. In the last column we give the total energy difference (in meV) with respect to the ground state in each case.

Bulk systems	Cell parameters (Å)			μ_{local} (μ_B)			ΔE (meV)
	a	b/a	c/a	μ_{Fe}	μ_{V}	μ_{H}	
Fe	2.88	1.00	1.00	2.33			
Fe+H (T)	3.10	0.97	0.98	2.52		-0.04	7
Fe+H (O)	2.76	1.00	1.30	2.47		-0.04	0
V	3.06	1.00	1.00		0.00		
V+H (O)	3.00	1.00	1.16		0.00		139
V+H (T)	3.17	1.00	1.00		0.00		0
B2 (Fe+V)	2.97	1.00	1.00	1.83	-0.89	0.00	
B2+H (T)	3.09	0.99	1.03	2.33	-0.40	0.01	247
B2+H (O1)	2.62	1.00	1.51	0.73	-0.34	0.00	67
B2+H (O2)	2.81	1.00	1.30	2.22	-0.62	0.00	0
B2+H (O1)	2.97	1.00	1.09	2.32	-0.60	0.03	585
B2+H (T)	2.97	1.00	1.07	2.00	-0.14	0.01	51
B2+H (O2)	2.97	1.00	1.08	1.91	0.04	-0.01	0

sistent with the instability of the tetragonally elongated regular octahedra. In the case of the H-loaded Fe bcc, the issue of the strong magnetic coupling is relevant. The insertion of H atoms leads to an increase in the Fe magnetic moment. In the T configuration the increase amounts to $0.15 \mu_B$ per Fe atom, while in the O configuration (with two inequivalent Fe atoms) the increase amounts to $0.13 \mu_B$ per Fe atom (see Table I).

Let us now discuss the trends for the B2 FeV alloy, which can be also viewed as a Fe_1/V_1 multilayer along the (001) direction. We have considered the H absorption, with a relative concentration of one H atom per unit cell, in different interstitial sites: the T site and the two O sites, as illustrated in Fig. 4. Here, the two O configurations differ as regards the local chemical environment. In the first one, referred to as O1, H is coordinated with four Fe atoms and two V atoms. In the second one, named O2, H is coordinated with two Fe atoms and four V atoms. H in the T configuration is coordinated with two Fe atoms and two V atoms. Two different structural optimizations have been performed. The first one consists in a relaxation of the unit cell so as to minimize the stress. In the second one, we simulate a pseudomorphic growth of the Fe_1/V_1 multilayer along the (001) direction by keeping fixed the in-plane interatomic distances ($a=b$) and relaxing the out-of-plane distance (c/a).

Let us first discuss the results obtained when relaxing the unit cell. In the H-free sample (Table I), the magnetic coupling between Fe and V is AP, with an average moment per atom of $0.95 \mu_B$, very similar to the value obtained in the Fe-V dimer ($1.0 \mu_B$), as well as to the value obtained through *ab initio* all-electron calculations by other authors at the interface of Fe/V multilayers.^{14,15} In Fig. 5 (left column)

and Table I we show the results after H insertion in the different interstitial sites. The configuration with H in O2 sites is the most stable one, with a total energy 67 meV lower than in the O1 sites and 247 meV lower than in the T sites.

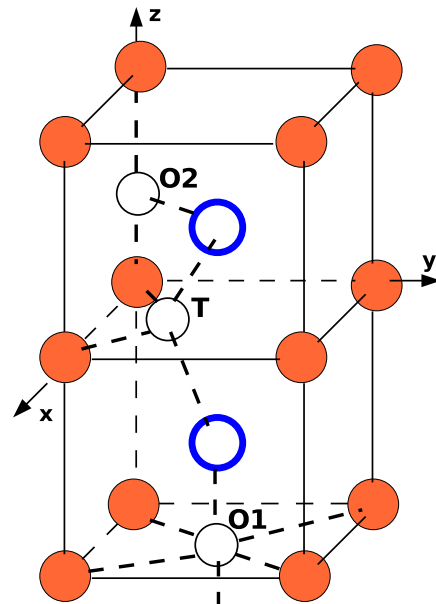


FIG. 4. (Color online) Illustration of the different interstitial positions of H upon absorption in the B2 FeV system. In the tetrahedral site (t), the H coordinates (in units of the cell parameter) are $(1/2 \ 1/4 \ 0)$. In the two different octahedral sites, referred to as O1 and O2, the H coordinates are $(1/2 \ 1/2 \ -1)$ and $(0 \ 0 \ 1/2)$, respectively. The O1 position is plotted with a shift of $-c$ not to be mistaken with the T insertion site.

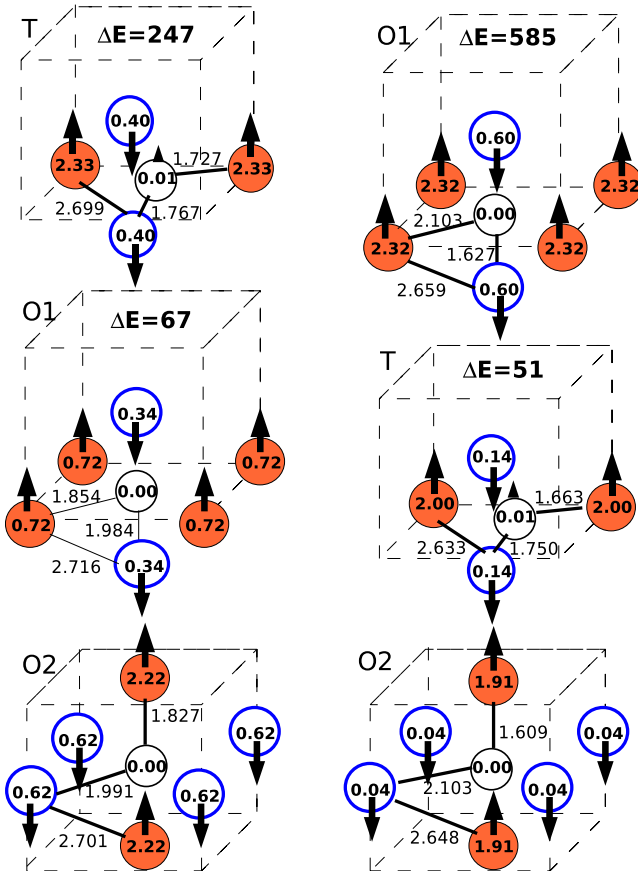


FIG. 5. (Color online) Structural and magnetic configurations obtained for the H-loaded FeV alloy with H in the different interstitial sites T, O1, and O2 (indicated on the top-left side of each configuration). Left column corresponds to the relaxation of the unit cell and right column to the relaxation, simulating a pseudomorphic growth of the Fe_1/V_1 multilayer along the (001) direction; that is by keeping fixed the in-plane interatomic distance and optimizing the out-of-plane distance. Orange filled, blue empty, and small black circles represent the Fe, V, and H atoms, respectively. Inside the circles are given the local magnetic moments in units of Bohr magneton and the couplings represented with arrows. In each column ΔE gives the total energy difference (in units of meV) with respect to the ground state (bottom of the column). Interatomic distances (in Å) are indicated between the circles representing the atoms. More information is provided in Table I.

This ground state is referred to as octahedral z site in the literature and is proposed to be the most stable position of H in Fe/V multilayers in the intermediate and high concentration limit according to elastic considerations derived from XRD data.¹¹ Notice that our investigated systems correspond to the high concentration limit ($x=1.0$). The preference of the octahedral sites in the alloy contrasts with the preference of the tetrahedral configuration in V bcc for this H concentration. It is pertinent to analyze the nature of the stress that can be either compressive or tensile. Due to the Fe-V lattice mismatch, the stress is compressive. The amount of H inserted in T sites within the V layers has been shown to depend on the epitaxial stress; the more compressive the stress, the lower the H insertion in T sites. Evidence of the influence of the stress comes out from the experiments on H-loaded

V/Fe and V/Mo multilayers. The relative concentration of H in T sites amounts to $x=0.15$ in the case of thin V films²⁹ on the Fe buffer (compressive stress), whereas it increases up to $x=0.25$ in the case of V/Mo multilayers³⁰ (tensile stress).

Coming now to the magnetic trends, the AP coupling between Fe and V is preserved after H insertion, as obtained in the freestanding clusters. For the ground state, H in O2 sites, as well as when H inserts in T sites, the magnetization increases as compared with the H-free alloy due to the enhancement of the Fe moments, while the magnetization decreases when H locates in the O1 sites. The Fe-V interatomic distances are larger upon H insertion, but when H locates in O1, the in-plane Fe-Fe distance (distance a , see Table I) is considerably shorter than in the other two configurations. In general, the shorter the in-plane Fe-Fe distance, the smaller the magnetic moment of the Fe atoms.

In order to simulate a pseudomorphic growth of the Fe_1/V_1 system along the (001) direction, as indicated previously, we have also performed the structural optimization by keeping fixed the in-plane interatomic distances $a=b$ and relaxing the out-of-plane distance (c/a). The value taken for $a=b=2.974$ Å corresponds to the average of the cell parameter of Fe bcc and V bcc as computed with SIESTA (Table I). As shown in Fig. 5 (right column) and Table I, now the distances are very similar whatever the H location within the system (T, O1, O2), which help us to extract conclusions about the preferential location of H as regard to its chemical environment. H prefers a rich-V environment since the stability of the system increases as H increases its V coordination relative to Fe. Thus, the O2 configuration is still the ground state, but followed now by the T configuration (51 meV less stable) and by the O1 one (585 meV less stable). Besides, the stability correlates with the increase in the Fe magnetic moments (see Fig. 5); that is, the more stable the configuration, the more noticeable the enhancement of the local moments on the Fe atoms as compared to the H-free alloy.

V. CONCLUSIONS

The effect of H on the structural and electronic properties of Fe-V systems has been investigated using the density-functional method SIESTA. Both finite and bulk systems have been investigated to better understand the general trends experimentally observed in H-loaded FeV systems. In the finite-size limit we have studied freestanding homonuclear and heteronuclear dimers with and without H, performing a full relaxation starting from all the possible initial structures. In the bulk and alloys, we have also performed a relaxation considering the H located in the different tetrahedral and octahedral interstitial sites.

The ground state of the homonuclear dimers has parallel (P) magnetic order while the Fe-V dimer has antiparallel (AP) magnetic order. For the H-loaded dimers, the following trends have been obtained: (i) the H atom stays in a V-rich environment; (ii) no change in the magnetic order in the dimers is obtained upon H loading; (iii) the H loading in the dimers leads to an increase in the interatomic distance and to an enhancement (reduction) of the local magnetic moment of

the Fe (V) atom. It is remarkable that these general trends are consistent with those experimentally observed in Fe/V multilayers.¹¹

Similar trends as those obtained in the freestanding clusters have been discussed in the bulk and alloys. Within V bcc, H is found to be absorbed preferentially in the tetrahedral site, which leads to an isotropic expansion of the unit cell, while the octahedral site is preferred in Fe bcc, accompanied by a large anisotropic expansion. In the B2 FeV alloy we have performed two different structural optimizations. The first one consists of a relaxation of the unit cell so as to minimize the stress and in the second one, we simulate a pseudomorphic growth of the Fe₁/V₁ multilayer along the (001) direction by keeping fixed the in-plane interatomic distances and relaxing the out-of-plane distance.

The magnetic coupling obtained between Fe and V in the H-free alloy is AP with an average moment per atom very similar to the value obtained in the Fe-V dimer, as well as to the value obtained by other authors at the interface of Fe/V multilayers. The ground state of the H-loaded alloy presents also AP coupling but the magnetization increases due to the enhancement of the Fe moment, as compared with the H-free alloy; H locates in an octahedral site, which maximizes its V coordination. This site, which is referred to as octahedral z site in the literature, is proposed to be the most stable posi-

tion of H in Fe/V multilayers in the intermediate and high concentration limit.¹¹ When the in-plane interatomic distances are kept fixed in the relaxation, the interatomic distances are very similar whatever the H location within the system. The stability of the system increases as H increases its V coordination relative to Fe. Besides, the stability correlates with the enhancement of the Fe magnetic moments; that is, the more stable the configuration, the more noticeable the enhancement of the Fe moments as compared to the H-free alloy.

The present study provides further support for the reliability of H loading as a means to improve the performance of Fe/V system in magnetic devices. We expect that our study will stimulate experimental investigations to confirm that the trends observed in H-loaded Fe/V multilayers are general and can be found in other geometrical environments such as in Fe-V clusters and other complex nanostructures.

ACKNOWLEDGMENTS

A.V. acknowledges the financial support and the kind hospitality from the University of Nantes, France. This work has been partially supported by the Spanish Ministry of Education and Science in conjunction with the European Regional Development Fund (Grant No. MAT2005-03415).

*Present address: Departamento de Física Teórica, Atómica y Óptica, Universidad de Valladolid, Spain.

- ¹P. Grünberg, R. Schreiber, Y. Pang, M. B. Brodsky, and H. Sowers, *Phys. Rev. Lett.* **57**, 2442 (1986).
- ²M. N. Baibich, J. M. Broto, A. Fert, F. Nguyen Van Dau, F. Petroff, P. Etienne, G. Creuzet, A. Friederich, and J. Chazelas, *Phys. Rev. Lett.* **61**, 2472 (1988).
- ³A. Vega, J. C. Parlebas, and C. Demangeat, *Handbook of Magnetic Materials* (North-Holland, Amsterdam, 2003), Vol. 15, p. 199.
- ⁴B. Skubic, E. Holmström, A. Bergman, and O. Eriksson, *Phys. Rev. B* **77**, 144408 (2008).
- ⁵B. Skubic, E. Holmström, D. Iusan, O. Bengone, O. Eriksson, R. Brucas, B. Hjörvarsson, V. Stanciu, and P. Nordblad, *Phys. Rev. Lett.* **96**, 057205 (2006).
- ⁶Ch. Rehm, H. Maletta, M. Fieber-Erdmann, E. Holub-Krappe, and F. Klose, *Phys. Rev. B* **65**, 113404 (2002).
- ⁷V. Leiner, K. Westerholt, A. M. Blixt, H. Zabel, and B. Hjörvarsson, *Phys. Rev. Lett.* **91**, 037202 (2003).
- ⁸D. Laberge, K. Westerholt, H. Zabel, and B. Hjörvarsson, *J. Magn. Magn. Mater.* **225**, 373 (2001).
- ⁹A. Mokrani, Ph.D. thesis, University of Strasbourg, 1988.
- ¹⁰A. C. Switendick, *Z. Phys. Chem., Neue Folge* **117**, 89 (1979).
- ¹¹G. Andersson, B. Hjörvarsson, and H. Zabel, *Phys. Rev. B* **55**, 15905 (1997).
- ¹²G. Andersson, B. Hjörvarsson, and P. Isberg, *Phys. Rev. B* **55**, 1774 (1997).
- ¹³T. Burkert, A. Miniotas, and B. Hjörvarsson, *Phys. Rev. B* **63**, 125424 (2001).
- ¹⁴A. M. N. Niklasson, B. Johansson, and H. L. Skriver, *Phys. Rev. B* **59**, 6373 (1999).
- ¹⁵J. Izquierdo, A. Vega, O. Elmouhssine, H. Dreyssé, and C. Demangeat, *Phys. Rev. B* **59** 14510 (1999).
- ¹⁶S. Ostanin, V. M. Uzdin, C. Demangeat, J. M. Wills, M. Alouani, and H. Dreyssé, *Phys. Rev. B* **61**, 4870 (2000).
- ¹⁷L.-C. Duda, P. Isberg, P. H. Andersson, P. Skytt, B. Hjörvarsson, J. H. Guo, C. Sathe, and J. Nordgren, *Phys. Rev. B* **55**, 12914 (1997).
- ¹⁸V. Meded, S. Olsson, P. Zahn, B. Hjörvarsson, and S. Mirbt, *Phys. Rev. B* **69**, 205409 (2004).
- ¹⁹V. Uzdin, D. Laberge, K. Westerholt, H. Zabel, and B. Hjörvarsson, *J. Magn. Magn. Mater.* **240**, 481 (2002).
- ²⁰J. M. Soler, E. Artacho, J. D. Gale, A. García, J. Junquera, P. Ordejon, and D. Sánchez-Portal, *J. Phys.: Condens. Matter* **14**, 2745 (2002).
- ²¹J. P. Perdew, K. Burke, and M. Ernzerhof, *Phys. Rev. Lett.* **77**, 3865 (1996).
- ²²N. Troullier and J. L. Martins, *Phys. Rev. B* **43**, 1993 (1991).
- ²³L. Kleinman and D. M. Bylander, *Phys. Rev. Lett.* **48**, 1425 (1982).
- ²⁴R. Robles, J. Izquierdo, A. Vega, and L. C. Balbas, *Phys. Rev. B* **63**, 172406 (2001).
- ²⁵G. Kresse and D. Joubert, *Phys. Rev. B* **59**, 1758 (1999).
- ²⁶J. Izquierdo, A. Vega, L. C. Balbas, D. Sanchez-Portal, J. Junquera, E. Artacho, J. M. Soler, and P. Ordejon, *Phys. Rev. B* **61**, 13639 (2000).
- ²⁷Steven G. Louie, Sverre Froyen, and Marvin L. Cohen, *Phys. Rev. B* **26**, 1738 (1982).
- ²⁸B. Hjörvarsson, C. Chacon, H. Zabel, and V. Leiner, *J. Alloys Compd.* **356-357**, 160 (2003).
- ²⁹J. Bloch, B. Hjörvarsson, S. Olsson, and R. Brukas, *Phys. Rev. B* **75**, 165418 (2007).
- ³⁰Stefan Olsson and Björgvin Hjörvarsson, *Phys. Rev. B* **71**, 035414 (2005).